Available online at www.sciencedirect.com
SCIENCE DIRECT®
Journal of Sound and Vibration 284 (2005) 133–149
JOURNAL OF SOUND AND VIBRATION
www.elsevier.com/locate/jsvi

Application of the arc-length method in nonlinear frequency response

J.V. Ferreira*, A.L. Serpa

Department of Computational Mechanics, Faculty of Mechanical Engineering, State University of Campinas, 13083-970 Campinas-SP, Brazil

Received 16 December 2002; accepted 8 June 2004
Available online 15 December 2004

Abstract

Several iterative numerical techniques have been developed to solve nonlinear structural problems and some of these methods are capable to trace complex paths in the space load/displacement. One of those most popular procedures is the arc-length method of Crisfield, which possesses the capability to overcome inflection points, without having the necessity of determining them. A great similarity exists between curves of the nonlinear load/displacement path obtained with the arc-length method, and curves of the frequency response of nonlinear dynamic systems. Both curves present limit points with snap-back and snap-through phenomena. This work consists of the description and the application of the arc-length method to solve a system of nonlinear equations obtaining as a result the nonlinear frequency response. The analysis employs the concept of the describing functions where the fundamental harmonic component is considered the most relevant and for some cases can be considered an approximation to the effect of all harmonics. Some examples involving a cubic stiffness and a gap nonlinearity are employed to illustrate the methodology.

1. Introduction

Although the various phenomena of nonlinear oscillations have long been recognized by many scientists, the practical solution of nonlinear problems has only been stimulated by the growing

*Corresponding author. Tel.: +55 19 3788 3195; fax: +55 19 3289 3722.
E-mail address: janito@fem.unicamp.br (J.V. Ferreira).

0022-460X/$ - see front matter © 2004 Elsevier Ltd. All rights reserved.
doi:10.1016/j.jsv.2004.06.025

development in computers. A large volume of investigation was carried out using the classical time domain techniques [1–3]. However, as a means of obtaining the steady-state response solution, these methods are very time consuming. Current efforts are directed towards the development of approximate frequency domain methods to seek approximate solutions for the nonlinear vibration problem. Many approximate frequency domain methods for determining the steady-state first-order harmonic response of structures use the describing function technique [4–10]. These methods normally use iterative methods for obtaining the solution. One of these iterative methods is the Newton–Raphson method which has been successfully applied to the analysis of many nonlinear systems. However, there are situations where their success has been limited, especially in the analysis presenting limit points with "snap-through" and "snap-back" behavior as shown in Fig. 1.

The first method capable of dealing with both cases of limit points (snap-back and snap-through) was the method proposed by Riks [11]. Crisfield [12] developed another approach to a continuous solution in the presence of snap-through behavior which is called the arc-length method.

The arc-length method together with the harmonic balance method was previously developed in Ref. [13] to compute forced response curves and applied to geometrically nonlinear beams. The harmonic balance method was also used to predict the dynamic response in the rotor/stator contact problem using the consistent arc-length approach [14,15], but both works present the main focus in the rotor/stator problem and did not discuss the computational implementation issues of the arc-length method in frequency response prediction.

This paper applies the arc-length method to dynamic problems to calculate the periodic response of a nonlinear system under periodic excitation and obtains as a result the nonlinear frequency response. The analysis employs the concept of describing functions where the fundamental harmonic component is considered the most relevant as it can give a good approximation to the effect of all harmonics. The paper also evaluates the robustness of the method on dynamic problems with localized nonlinearities. The main purpose of this work is to

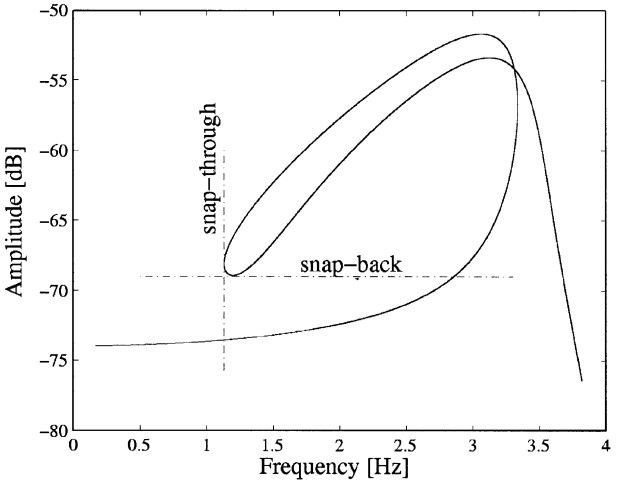

Fig. 1. Snap-through and snap-back phenomena.

present how the frequency response can be determined for strong nonlinearities, for example, cubic stiffness, gaps and friction, which leads to the usual snap-back and snap-through behavior, using the non-consistent arc-length method and to discuss the formulation and the implementation details.

2. Nonlinear dynamic analysis of mechanical systems

2.1. Fundamental harmonic analysis

The matrix differential equation of motion for a nonlinear structure subject to an external excitation $\mathbf{f}_e$ having internal localized nonlinear forces, $\mathbf{f}$, can be written as

$$\mathbf{M}\ddot{\mathbf{x}} + \mathbf{C}\dot{\mathbf{x}} + \mathbf{K}\mathbf{x} + \mathbf{f} = \mathbf{f}_e, \tag{1}$$

where $\mathbf{M}$ is the mass matrix, $\mathbf{C}$ is the viscous damping matrix, and $\mathbf{K}$ is the stiffness matrix.

Assuming the external excitation as a sinusoidal excitation, $\mathbf{f}_e$ can be written as

$$\mathbf{f}_e(t) = \mathbf{F}_e e^{i\omega t} + \mathbf{F}_e^* e^{-i\omega t} = \mathbf{F}_e e^{i\tau} + \mathbf{F}_e^* e^{-i\tau}, \tag{2}$$

where $\mathbf{F}_e$ represents the excitation amplitude, ω is the excitation frequency, $\tau = \omega t$, and the superscript $*$ denotes the complex conjugate.

The steady-state solution can be represented by a Fourier series [16] as

$$\mathbf{x}(t) = \sum_{m=0}^{\infty} \mathbf{x}^m(t) = \sum_{m=-\infty}^{\infty} \mathbf{X}^m e^{im\omega t} = \sum_{m=-\infty}^{\infty} \mathbf{X}^m e^{im\tau}, \tag{3}$$

where m is the harmonic order and $\mathbf{X}$ is the complex displacement amplitude. Note that $\mathbf{X}^{-m}$ is the complex conjugate of $\mathbf{X}^m$, which results in real harmonic components:

$$\mathbf{x}^m(t) = \mathbf{X}^m e^{im\tau} + \mathbf{X}^{-m} e^{-im\tau}. \tag{4}$$

When the higher harmonic terms of the response have small amplitudes relative to the fundamental component, the response is dominated by the fundamental component of the Fourier series for $\mathbf{x}(t)$ denoted by $\mathbf{x}^1(t)$. Thus, the response $\mathbf{x}(t)$ can be written as

$$\mathbf{x}(t) \approx \mathbf{x}^1(t) = \sum_{m=-1}^{1} \mathbf{X}^m e^{im\tau}. \tag{5}$$

The approximate response at a general coordinate j can be written as

$$x_j \approx x_j^1 = \sum_{m=-1}^{1} X_j^m e^{im\tau}, \tag{6}$$

where the X_j^{-1} and X_j^1 are the "complex displacement amplitudes" related to the fundamental component and related to coordinate j. Since X_j^{-1} and X_j^1 are complex conjugates, the next developments in this paper will be performed in terms of X_j^1 only.

The complex displacement response X_j^1 can be written in terms of magnitude and phase:

$$X_j^1 = \bar{X}_j^1 e^{i\phi_j^1}, \tag{7}$$

where $\bar{X}$ is the magnitude and ϕ is the phase angle.

Similarly, the inter-coordinate relative displacement response y between coordinates k and l can be represented as

$$y_{kl} = x_k - x_l \approx y_{kl}^1 = Y_{kl}^1 e^{i\tau}, \tag{8}$$

$$Y_{kl}^1 = \bar{Y}_{kl}^1 e^{i\alpha_{kl}^1} = X_k^1 - X_l^1 \quad (k \neq l), \tag{9}$$

where $\bar{Y}_{kl}^1$ is the complex inter-coordinate relative displacement magnitude and α_{kl}^1 is the respective phase angle.

The assumed solution y_{kl} in Eq. (8) can be inserted in the nonlinear function resulting in nonlinear forces $f_{kl}(y_k^1)$ and $f_{kl}(y_l^1)$, that can be denoted as $f_{k,l}(y_{kl}^1)$, and can also be expanded by a Fourier series and expressed in complex form as

$$f_{k,l}(y_{kl}^1) = \sum_{m=-\infty}^{\infty} \mathscr{F}_{k,l}^m e^{im\tau}, \tag{10}$$

where

$$\mathscr{F}_{k,l}^m = \bar{\mathscr{F}}_{k,l}^m e^{i\varphi^m}, \tag{11}$$

with $\bar{\mathscr{F}}_{k,l}^m$ and φ^m representing again the complex magnitude and phase angle, respectively.

The terms of Eq. (11) can be calculated using Fourier Series as

$$\mathscr{F}_{k,l}^0 = \frac{1}{2\pi}\int_0^{2\pi} f_{k,l}(y_{kl}^1)\,d\tau, \quad \mathscr{F}_{k,l}^m = \frac{1}{\pi}\int_0^{2\pi} f_{k,l}(y_{kl}^1)e^{-im\tau}\,d\tau \quad (m \geqslant 1). \tag{12}$$

Assuming now that the nonlinear force $f_{k,l}(y_{kl}^1)$ is also dominated by its fundamental term, then the approximate nonlinear force $\tilde{f}_{k,l}^1(y_{kl}^1)$ can be written as

$$f_{k,l}(y_{kl}^1) \approx \tilde{f}_{k,l}^1(y_{kl}^1) = \sum_{m=-1}^{1} \mathscr{F}_{k,l}^1 e^{i\tau} = \sum_{m=-1}^{1} (A_{kl}^1 \sin(\tau) + B_{kl}^1 \cos(\tau)), \tag{13}$$

where

$$A_{kl}^1 = \frac{1}{\pi}\int_0^{2\pi} f_{k,l}(y_{kl}^1)\sin\tau\,d\tau, \quad B_{kl}^1 = \frac{1}{\pi}\int_0^{2\pi} f_{k,l}(y_{kl}^1)\cos\tau\,d\tau.$$

Again as the $\mathscr{F}_{k,l}^{-1}$ and $\mathscr{F}_{k,l}^1$ are the complex conjugate forces, the next developments will be performed in terms of $\mathscr{F}_{k,l}^1$ only.

The component $\mathscr{F}_{k,l}^1$ of the approximated nonlinear force $\tilde{f}_{k,l}(\tilde{y}_{kl})$ can be written as

$$\mathscr{F}_{k,l}^1 = v_{kl}^1 Y_{kl}^1, \tag{14}$$

where v_{kl}^1 is the known describing function [17] expressed as

$$v_{kl}^1 = \frac{\mathscr{F}_{k,l}^1}{Y_{kl}^1}. \tag{15}$$

Eq. (14) can be expressed in terms of the general coordinates as

$$\begin{Bmatrix} \mathscr{F}_k^1 \\ \mathscr{F}_l^1 \end{Bmatrix} = \begin{bmatrix} v_{kl}^1 & -v_{kl}^1 \\ -v_{kl}^1 & v_{kl}^1 \end{bmatrix} \begin{Bmatrix} X_k^1 \\ X_l^1 \end{Bmatrix} = \mathbf{\Theta}_{kl}^1 \begin{Bmatrix} X_k^1 \\ X_l^1 \end{Bmatrix}, \tag{16}$$

with

$$\mathbf{\Theta}_{kl}^1 = \begin{bmatrix} v_{kl}^1 & -v_{kl}^1 \\ -v_{kl}^1 & v_{kl}^1 \end{bmatrix} \tag{17}$$

being the describing function matrix.

2.2. Impedance equation

After describing the excitation force, the nonlinear force and the response by their fundamental harmonic components, it is possible to rewrite Eq. (1) in the frequency domain as two complex conjugate equations in terms of $\mathbf{X}^1$ and $\mathbf{X}^{-1}$, respectively.

Again, since $\mathbf{X}^1$ and $\mathbf{X}^{-1}$ are complex conjugate, the next developments are performed in terms of $\mathbf{X}^1$. The equation for $\mathbf{X}^1$ is

$$\mathbf{M}(-\omega^2\mathbf{X}^1) + \mathbf{C}\mathrm{i}\omega\mathbf{X}^1 + \mathbf{K}\mathbf{X}^1 + \mathscr{F}^1 = \mathbf{F}_e. \tag{18}$$

Eq. (18) can be written in impedance form as

$$\mathbf{Z}(\omega, \mathbf{X})\mathbf{X}^1 = \mathbf{F}_e, \tag{19}$$

where

$$\mathbf{Z}(\omega, \mathbf{X}) = \mathbf{K} - \mathbf{M}\omega^2 + \mathrm{i}\omega\mathbf{C} + \mathbf{\Theta}^1(\mathbf{X}^1) \tag{20}$$

and

$$\mathscr{F}^1 = \mathbf{\Theta}^1\mathbf{X}^1, \tag{21}$$

as a generalization of Eq. (16), making explicit the use of the describing function matrix $\mathbf{\Theta}^1$.

3. Nonlinear frequency response calculation using the arc-length method

3.1. Basic theory of solution

The usual application of the arc-length method in nonlinear static equilibrium problems considers displacement and load level as parameters [18]. This section adapts the arc-length method to obtain the nonlinear frequency response in terms of the excitation frequency and

displacement amplitude. Therefore, Eq. (19) can be written in residual form as

$$\mathbf{\Psi}(\mathbf{X}, \lambda\omega) = \mathbf{X} - \mathbf{H}(\mathbf{X}, \lambda\omega)\mathbf{F}_e = \mathbf{X} - \mathbf{Z}(\mathbf{X}, \lambda\omega)^{-1}\mathbf{F}_e, \tag{22}$$

where

$$\mathbf{Z}(\mathbf{X}, \lambda\omega) = \mathbf{K} - \mathbf{M}\lambda^2\omega^2 + \mathrm{i}\lambda\omega\mathbf{C} + \mathbf{\Theta}(\mathbf{X}) = \mathbf{H}(\mathbf{X}, \lambda\omega)^{-1} \tag{23}$$

and the scalar λ is a "frequency-level parameter", in this case equivalent to the load level parameter of nonlinear static analysis [18]. Notice that the superscript 1 related to the first harmonic is omitted in order to simplify the notation.

The arc-length method is described within the category of continuation methods and it is applied to obtain solution paths. Basically, the arc-length method first considers the frequency factor λ as a variable in the residual equation (22). Then, an extra new constraint equation is added to the residual equilibrium equation (22) for defining unequivocally the next equilibrium point solution at an intersection between the solution path and the constraint equation. Finally the nonlinear extended system is then solved using standard iterative techniques to obtain the equilibrium point solution.

The spherical constraint equation proposed by Crisfield [18] in the general format can be adapted to the frequency response determination as

$$a(\Delta\mathbf{X}, \Delta\lambda) = (\Delta\mathbf{X}^t\Delta\mathbf{X} + \Delta\lambda^2\psi^2\omega^2) - \Delta l^2 = 0, \tag{24}$$

where Δl is the fixed radius of the desired intersection, the scalar ψ is a scale parameter, the vector $\Delta\mathbf{X}$ and the scalar $\Delta\lambda$ are the incremental displacement and frequency factor, respectively, i.e.,

$$\Delta\mathbf{X} = \mathbf{X} - \mathbf{X}^{(i)}, \quad \Delta\lambda = \lambda - \lambda^{(i)}, \tag{25,26}$$

with $\mathbf{X}^{(i)}$ corresponding to the last known/converged equilibrium point and $\lambda^{(i)}$ is initialized as one, corresponding to a full frequency initial step.

An extended system collecting the equilibrium equation (22) and the constraint equation (24) can be rewritten as

$$\begin{Bmatrix} \mathbf{\Psi}(\mathbf{X}, \lambda\omega) \\ a(\Delta\mathbf{X}, \Delta\lambda) \end{Bmatrix} = \begin{Bmatrix} \mathbf{X} - \mathbf{H}(\mathbf{X}, \lambda\omega)\mathbf{F} \\ (\Delta\mathbf{X}^t\Delta\mathbf{X} + \Delta\lambda^2\psi^2\omega^2) - \Delta l^2 \end{Bmatrix} = \{\mathbf{0}\}. \tag{27}$$

For a known position along the solution path $(\mathbf{X}^{(i)}, \lambda^{(i)}\omega)$, it is possible to visualize geometrically Eq. (27) for a one-degree of freedom system. Fig. 2 shows the intersection of both curves related with Eq. (27), highlighting the next possible solutions.

Eq. (27) represents a nonlinear system of $n+1$ unknowns which can be solved by standard incremental-iterative procedures, such as Newton–Raphson or modified Newton–Raphson techniques to obtain the solution point along the path. These methods usually require suitable starting values for the iteration procedure to converge to the correct solution points.

The arc-length procedure that obtains the next equilibrium point $(\mathbf{X}^{(i+1)}, \lambda^{(i+1)}\omega)$ normally consists of two phases, the prediction phase and the correction phase. The predictor procedures are applied to estimate the first solution to determine the direction of the path to be followed. The corrector iterative procedures are used for computing a convergence sequence of estimates to obtain the converged solution. The prediction and correction iterations are denoted by the superscript k.

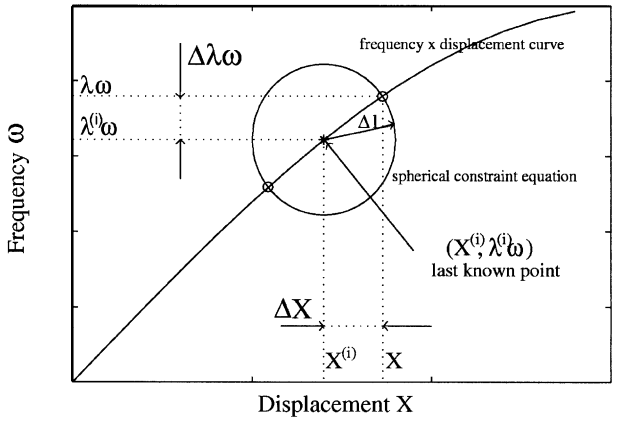

Fig. 2. Solution path and the constraint equation curve.

3.2. Predictor procedure

The direction to be followed can be determined by the point obtained by a predictor procedure given by

$$\Delta\mathbf{X}^{(0)} = -\Delta\lambda^{(0)}\mathbf{K}_t^{(0)^{-1}}\mathbf{q}, \tag{28}$$

where $\mathbf{K}_t = \partial\boldsymbol{\Psi}/\partial\mathbf{X}$ plays the same role of the tangent stiffness matrix of a static nonlinear analysis, and $\mathbf{q} = \partial\boldsymbol{\Psi}/\partial\lambda$.

Eq. (28) is an approximation of Eq. (40) considering that the iterations start from a converged equilibrium solution where $\boldsymbol{\Psi} = \mathbf{0}$. The expressions of Section 3.3 show how to obtain Eq. (40).

Substituting the prediction of Eq. (28) into the constraint equation (24) gives

$$\Delta\lambda^{(0)} = \pm\frac{\Delta l}{\sqrt{(\mathbf{K}_t^{-1}\mathbf{q})^t(\mathbf{K}_t^{-1}\mathbf{q}) + \psi^2\omega^2)}}. \tag{29}$$

From Eq. (29) it is possible to see that because of the plus or minus signal, two solutions are available. If the sign is not chosen appropriately, the direction for searching the next point is incorrect and the corrector phase may converge to an undesired point, travelling back to the previously computed solution.

There are many criteria proposed in the literature to determine the sign of Eq. (29) [18–23], but practical experience from many researches suggests that the criterion which uses the sign of the determinant of the matrix $|\mathbf{K}_t|$, to determine the sign of the initial frequency increment $\Delta\lambda$, i.e., $\text{sign}\,|\mathbf{K}_t| = \text{sign}\,\Delta\lambda$, works quite well in most cases [18,23–25], although some unsuccessful cases have also been reported [26,27].

As a result of the predictor phase, $\mathbf{X}^{(k)}$ and $\lambda^{(k)}$ are obtained according to the following equations:

$$\mathbf{X}^{(k)} = \mathbf{X}^{(i)} + \Delta\mathbf{X}^{(0)}, \quad \lambda^{(k)} = \lambda^{(i)} + \Delta\lambda^{(0)}. \tag{30}$$

3.3. Corrector procedure

In the correction phase, a numerical procedure is applied to find the solution of the extended system of Eq. (27), with the initial guess $(\mathbf{X}^{(k)}, \lambda^{(k)}\omega)$ determined on the predictor phase. It is convenient to linearize either the extended equation or both Eqs. (22) and (24), by applying the Taylor series, leading to

$$\boldsymbol{\Psi} = \boldsymbol{\Psi}_0 + \frac{\partial \boldsymbol{\Psi}}{\partial \mathbf{X}}\,\delta\mathbf{X} + \frac{\partial \boldsymbol{\Psi}}{\partial \lambda}\,\delta\lambda = \boldsymbol{\Psi}_0 + \mathbf{K}_t\delta\mathbf{X} + \mathbf{q}\delta\lambda = 0, \tag{31}$$

$$a = a_0 + \frac{\partial a}{\partial \mathbf{X}}\,\delta\mathbf{X} + \frac{\partial a}{\partial \lambda}\,\delta\lambda = a_0 + 2\Delta\mathbf{X}^t\delta\mathbf{X} + 2\Delta\lambda\,\delta\lambda\,\psi^2\omega^2 = 0, \tag{32}$$

where

$$\mathbf{K}_t = \frac{\partial \boldsymbol{\Psi}}{\partial \mathbf{X}}, \quad \mathbf{q} = \frac{\partial \boldsymbol{\Psi}}{\partial \lambda}, \tag{33,34}$$

$$\frac{\partial a}{\partial \mathbf{X}} = 2\Delta\mathbf{X}^t\,\frac{\partial \Delta\mathbf{X}}{\partial \mathbf{X}} = 2\Delta\mathbf{X}^t\delta\mathbf{X}, \tag{35}$$

$$\frac{\partial a}{\partial \lambda} = 2\Delta\lambda\,\delta\lambda\,\psi^2\omega^2\,\frac{\partial \Delta\lambda}{\partial \lambda} = 2\Delta\lambda\,\delta\,\lambda\,\psi^2\omega^2. \tag{36}$$

It is important to note that in Eq. (31), both terms, $\partial\boldsymbol{\Psi}/\partial\mathbf{X}$ and $\partial\boldsymbol{\Psi}/\partial\lambda$, must be calculated from the residual equation (22). In this work, both derivatives were calculated numerically using finite differences with a perturbation parameter of 1×10^{-8}.

Finally, combining Eqs. (31) and (32) to solve for $\delta\mathbf{X}$ and $\delta\lambda$, the nonlinear extend system can be written as

$$\begin{pmatrix} \delta\mathbf{X} \\ \delta\lambda \end{pmatrix} = -\begin{bmatrix} \mathbf{K}_t & \mathbf{q} \\ 2\Delta\mathbf{X}^t & 2\Delta\lambda\,\psi^2\omega^2 \end{bmatrix}^{-1} \begin{pmatrix} \boldsymbol{\Psi}_0 \\ a_0 \end{pmatrix}. \tag{37}$$

Eq. (37) can be solved using standard iterative techniques to obtain the solution $(\delta\mathbf{X}, \delta\lambda)$. This procedure is known as consistent method. However, the augmented stiffness matrix within the brackets in Eq. (37) is neither symmetric nor banded. This problem can be overcome by adopting the non-consistent scheme, where the original augmented system to be solved at each iteration, Eq. (37), is replaced by the equations

$$[\mathbf{K}_t^{(k)}\mathbf{q}]\begin{pmatrix} \delta\mathbf{X}^{(k+1)} \\ \delta\lambda^{(k+1)} \end{pmatrix} = -\boldsymbol{\Psi}(\mathbf{X}^{(k)}, \lambda^{(k)}) = -\boldsymbol{\Psi}^{(k)}, \tag{38}$$

$$\Delta\mathbf{X}^{(k+1)^t}\Delta\mathbf{X}^{(k+1)} + \Delta\lambda^{(k+1)^2}\psi^2\omega^2 = \Delta l^2, \tag{39}$$

where $\mathbf{K}_t^{(k)} = \mathbf{K}_t(\mathbf{X}^{(k)})$.

Solution of Eqs. (38) and (39) converges to the same equilibrium solution $(\delta\mathbf{X}, \delta\lambda)$ of Eq. (37).

The process for solving by a non-consistent method starts with Eq. (38) where the iterative displacement vector, $\delta\mathbf{X}^{(k+1)}$, can be obtained as

$$\delta\mathbf{X}^{(k)} = -\mathbf{K}_t^{(k)^{-1}}\boldsymbol{\Psi}^{(k)} - \delta\lambda^{(k)}\mathbf{K}_t^{(k)^{-1}}\mathbf{q}. \tag{40}$$

Eq. (40) can be rewritten as

$$\delta\mathbf{X}^{(k)} = \delta\bar{\mathbf{X}}^{(k)} + \delta\lambda^{(k)}\delta\mathbf{X}_t^{(k)}, \tag{41}$$

where $\delta\bar{\mathbf{X}}^{(k)}$ is the iterative displacement vector that would result from a standard frequency-controlled algorithm (Newton–Raphson, Newton–Raphson modified, etc.) at a fixed frequency level $\delta\lambda^{(k)}$, i.e.,

$$\delta\bar{\mathbf{X}}^{(k)} = -\mathbf{K}_t^{(k)^{-1}}\boldsymbol{\Psi}^{(k)} \tag{42}$$

and $\delta\mathbf{X}_t^{(k)}$ is the displacement vector corresponding to the fixed frequency ω, also known as tangential solution:

$$\delta\mathbf{X}_t^{(k)} = -\mathbf{K}_t^{(k)^{-1}}\mathbf{q}. \tag{43}$$

Having determined the expression for the iterative displacement vector, $\delta\mathbf{X}^{(k)}$, where the $\delta\lambda^{(k)}$ is still unknown, it is possible to write the new incremental displacement $\Delta\mathbf{X}^{(k+1)}$ as

$$\Delta\mathbf{X}^{(k+1)} = \Delta\mathbf{X}^{(k)} + \delta\mathbf{X}^{(k)}. \tag{44}$$

Substitution of Eq. (41) into Eq. (44) leads to

$$\Delta\mathbf{X}^{(k+1)} = \Delta\mathbf{X}^{(k)} + \delta\bar{\mathbf{X}}^{(k)} + \delta\lambda^{(k)}\delta\mathbf{X}_t^{(k)}, \tag{45}$$

where $\delta\lambda^{(k)}$ is the only unknown.

The incremental frequency factor can be similarly written as

$$\Delta\lambda^{(k+1)} = \Delta\lambda^{(k)} + \delta\lambda^{(k)}. \tag{46}$$

Substitution of Eq. (45) into the restriction equation (39) leads to the scalar quadratic equation

$$a\delta\lambda^{(k)^2} + b\delta\lambda^{(k)} + c = 0, \tag{47}$$

where

$$\begin{aligned} a &= \delta\mathbf{X}_t^{(k)^t}\delta\mathbf{X}_t^{(k)} + \psi^2\omega^2, \\ b &= 2\delta\mathbf{X}_t^{(k)^t}(\Delta\mathbf{X}^{(k)} + \delta\bar{\mathbf{X}}^{(k)}) + 2\Delta\lambda^{(k)}\psi^2\omega^2, \\ c &= (\Delta\mathbf{X}^{(k)} + \delta\bar{\mathbf{X}}^{(k)})^t(\Delta\mathbf{X}^{(k)} + \delta\bar{\mathbf{X}}^{(k)}) - \Delta l^2 + \Delta\lambda^{(k)^2}\psi^2\omega^2. \end{aligned}$$

The iterative frequency factor $\delta\lambda^{(k)}$ can be determined by choosing the appropriate root to the quadratic equation (47). The right root is normally chosen by computing both solutions:

$$\Delta\mathbf{X}_1^{(k+1)} = \Delta\mathbf{X}^{(k)} + \delta\bar{\mathbf{X}}^{(k)} + \delta\lambda_1^{(k)}\delta\mathbf{X}_t^{(k)}, \tag{48}$$

$$\Delta\mathbf{X}_2^{(k+1)} = \Delta\mathbf{X}^{(k)} + \delta\bar{\mathbf{X}}^{(k)} + \delta\lambda_2^{(k)}\delta\mathbf{X}_t^{(k)} \tag{49}$$

and then choosing the solution that yields the minimum angle between $\Delta\mathbf{X}_{1,2}^{(k+1)}$ and $\Delta\mathbf{X}^{(k)}$ [18], i.e., the maximum cosine of the angle given by the equation

$$\cos\theta = \frac{\Delta\mathbf{X}_{1,2}^{(k+1)}\Delta\mathbf{X}^{(k)}}{\Delta l^2}. \tag{50}$$

Numerical experiments revealed that this criteria works well for most cases. Therefore, other criteria are object of research in order to increase robustness of the method.

Having achieved the iterative frequency factor $\delta\lambda^{(k)}$, the iterative displacement, $\delta\mathbf{X}^{(k)}$, would be computed by Eq. (41). Then the incremental displacement would be computed by Eq. (44) and the incremental frequency factor by Eq. (46).

When the incremental displacement, Eq. (44), and incremental frequency factor, Eq. (46), are added to the displacement and frequency level of the previous converged point, $(\mathbf{X}^{(k)}, \lambda^{(k)}\omega)$ lead to the point $(\mathbf{X}^{(k+1)}, \lambda^{(k+1)}\omega)$. Repeating this process and using a convergence criterion to stop the process, a solution $(\Delta\mathbf{X}, \Delta\lambda)$ is obtained. This solution leads to the next converged point that lays on the intersection of the constraint equation and the path:

$$\mathbf{X} = \mathbf{X}^{(i+1)} = \mathbf{X}^{(i)} + \Delta X, \quad \lambda = \lambda^{(i+1)} = \lambda^{(i)} + \Delta\lambda, \quad \omega = \omega^{(i+1)} = \lambda\omega^{(i)}. \tag{51}$$

3.4. Automatic radius length

The size of the radius used on the arc-length method is a crucial point for achieving a robust method. Once the predictor has been obtained and the direction is determined, it is desired that only one solution remains in that direction. If the radius is too large, it may be possible to have more than one solution along that path, which means that the constraint equation has intersected other portions of the solution path. On the other hand, if the radius is chosen too small, the computational cost to obtain the solution path is very expensive. A simple technique was proposed by Crisfield [18], where the incremental radius is given by the equation

$$\Delta l^{(k+1)} = \Delta l^{(k)}\left(\frac{I_d}{I^{(k)}}\right), \tag{52}$$

where $\Delta l^{(k+1)}$ and $\Delta l^{(k)}$ are the radius on the iteration $k+1$ and k, I_d is the input desired iterations and $I^{(k)}$ is the number of the iteration required on the iteration k.

The above radius control leads to the provision of small increments when the response is most nonlinear and large increments when the response is most linear. Although this has been working very well for the tests so far realized, certain deficiencies have been reported when handling problems with sudden changes of solution path [26,28].

3.5. Estimating the initial radius length

The necessity of estimating the initial radius Δl comes from the fact that the user usually has little idea of an appropriate magnitude to be chosen. Therefore, a solution must be applied to obtain a starting radius compatible with the frequency applied. A suitable starting value can be obtained by first specifying the initial frequency increment $\Delta\lambda$ and then calculating the Newton

step $\delta\mathbf{X}$ from the initial known point $(\mathbf{X}^{(0)}, \lambda^{(0)}\omega)$ as

$$\delta\mathbf{X} = -\mathbf{K}_t^{(0)^{-1}}\boldsymbol{\Psi}(\mathbf{X}^{(0)}, \lambda^{(0)} + \Delta\lambda). \tag{53}$$

Finally, the starting radius length can be calculated by

$$\Delta l = \sqrt{\delta\mathbf{X}^t\delta\mathbf{X}}. \tag{54}$$

The estimate of the initial frequency increment $\Delta\lambda$ can be performed using the physical insight of the problem.

3.6. Solving the complex load factor

The frequency factor increment calculated from Eq. (47) can produce real or complex roots. When the roots are complex, it means that the arc-length constraint equation fails to determine the next frequency factor increment over the restriction. To prevent this kind of failure, Zhou and Murray [29] proposed a relaxation factor to minimize the failure. Experience showed that applying this relaxation method for many degrees of freedom, minimizes the failure, but does not solve the problem completely. The strategy adopted by Crisfiled [18] of reducing the radius and restarting from the last converged point worked very well for all the cases tested in this work.

4. Numerical tests

In this section, two examples, both exhibiting strong snap-through and snap-back behaviors, were selected to examine the performance of the arc-length method for obtaining the nonlinear frequency response. A key feature of the present problems is the fact that the frequency-deflection curves or specifically amplitude–frequency curves are characterized by "snap-throughs" and "snap-backs". This makes the present analysis particularly suited for the proposed verification. Also in this work, the scale parameter ψ of Eq. (24) was adopted as 0 for both examples, representing the particular case of the cylindrical arc-length method [18].

The first-order frequency response was obtained as a result in the simulations. It is an extension of the frequency response functions of linear structures to nonlinear structures. In the cases studied, a pure sinusoidal excitation was used and the first-order frequency response function H^{11} of a nonlinear structure can be defined as the spectral ratio of the response x_i and the force f_{ej} at the frequency of excitation, ω, written as

$$H_{ij}^{11}(\omega) = \frac{X_i^1}{F_{ej}^1}. \tag{55}$$

In this case, only the fundamental frequency component of the response x composed of the fundamental frequency is retained and all the subharmonics, superharmonics and combinations of both are ignored.

4.1. Cubic stiffness

The first simulation consists of obtaining the solution path of an equation of the assembled structure of Fig. 3 with three nonlinear cubic stiffness elements, denoted as f_1, f_2 and f_3.

The function that represents the force of the nonlinear elements is given by

$$f = Ky + \beta y^3. \tag{56}$$

The physical characteristics of the system are taken to be: $M_1 = 2\,\text{kg}$, $M_2 = 1\,\text{kg}$, $M_3 = 1.5\,\text{kg}$, $c_1 = 2.5\,\text{Nm/s}$, $c_2 = 0.3\,\text{Nm/s}$, $c_3 = 0.08\,\text{Nm/s}$, $K_1 = 5 \times 10^3\,\text{N/m}$, $K_2 = 2 \times 10^3\,\text{N/m}$, $K_3 = 4 \times 10^3\,\text{N/m}$, $\beta_1 = -4\,\text{N/m}$, $\beta_2 = -4\,\text{N/m}$, $\beta_3 = -4\,\text{N/m}$.

The arc-length method was used to solve the problem and the initial radius used was equivalent to 6 mm. The amplitude and phase of the frequency response H_{11}^{11} for three levels of force f_e (0.1, 0.5 and 2.0 N) are shown in Figs. 4 and 5.

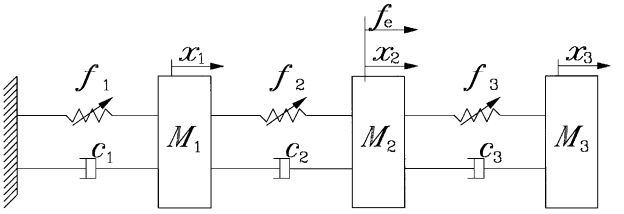

Fig. 3. Assembled structure (first example).

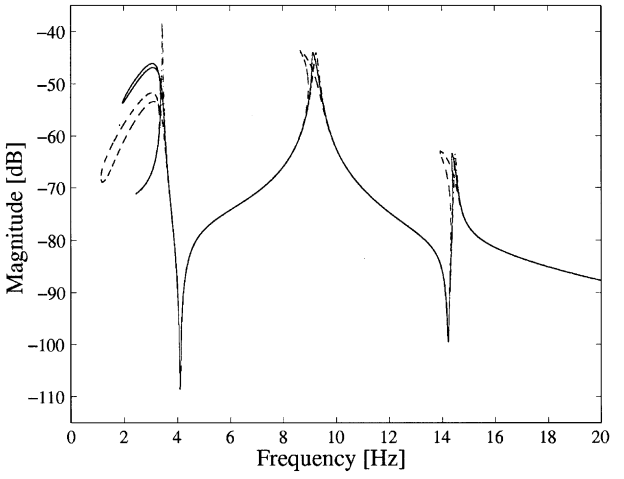

Fig. 4. Frequency response magnitude H_{11}^{11} for 0.1 N (– –) force, for 1.0 N (–) force and for 4.0 N (–·–) force (related to the structure of Fig. 3).

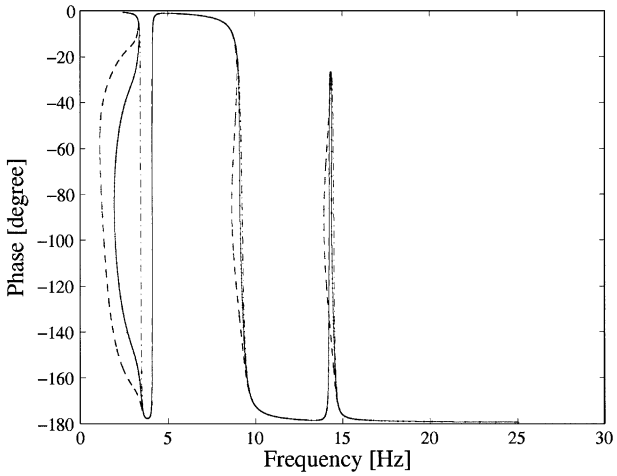

Fig. 5. Frequency response phase H_{11}^{11} for 0.1 N (––) force, for 1.0 N (–) force and for 4.0 N (–·–) force (related to the structure of Fig. 3).

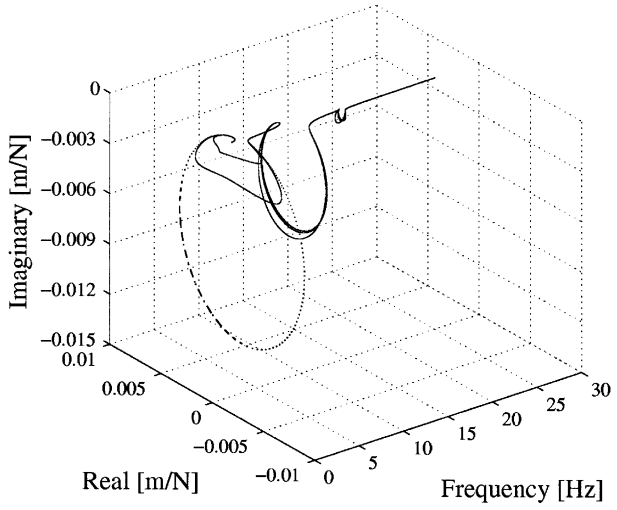

Fig. 6. Frequency response H_{11}^{11} for 0.1 N (––) force, for 1.0 N (–) force and for 4.0 N (–·–) force (related to the structure of Fig. 3).

A three-dimension plot is used to visualize the frequency response H_{11}^{11} and is shown in Fig. 6.

4.2. Gap

The second simulation consists of obtaining the solution path of an equation of the assembled structure of Fig. 7 with three nonlinear gap elements, denoted as gap_1, gap_2 and gap_3.

The function that represents the force of the nonlinear elements is given by

$$f = \begin{cases} 0 & \text{if } -\text{gap} < y < \text{gap}, \\ k(y-\text{gap}) & \text{if } y \geqslant \text{gap}, \\ k(y+\text{gap}) & \text{if } y \leqslant -\text{gap} \end{cases} \tag{57}$$

and the plot of the respective function can be seen in Fig. 8.

The physical characteristics of the system are taken to be: $M_1 = 2\,\text{kg}$, $M_2 = 1\,\text{kg}$, $M_3 = 1.5\,\text{kg}$, $c_1 = 2.5\,\text{Nm/s}$, $c_2 = 0.3\,\text{Nm/s}$, $c_3 = 0.08\,\text{Nm/s}$, $K_1 = 5 \times 10^3\,\text{N/m}$, $K_2 = 2 \times 10^3\,\text{N/m}$, $K_3 = 4 \times 10^3\,\text{N/m}$, $k_1 = 10000\,\text{N/m}$, $k_2 = 10000\,\text{N/m}$, $k_3 = 10000\,\text{N/m}$, $\text{gap}_1 = 2\,\text{mm}$, $\text{gap}_2 = 4\,\text{mm}$, $\text{gap}_3 = 6\,\text{mm}$.

The arc-length method was used to solve the problem and the initial radius used was equivalent to 6 mm. The amplitude and phase of the frequency response H_{11}^{11} for three levels of force f_e (0.1, 1.0 and 4.0 N) are shown in Figs. 9 and 10.

The three-dimension plot of the frequency response H_{11}^{11} is shown in Fig. 11.

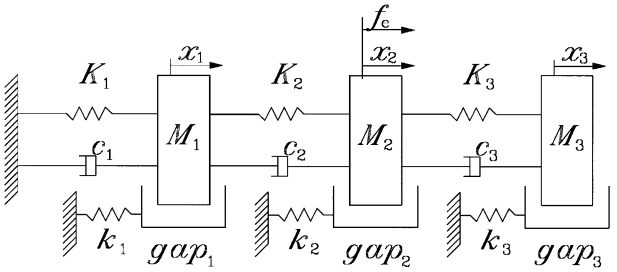

Fig. 7. Assembled structure (second example).

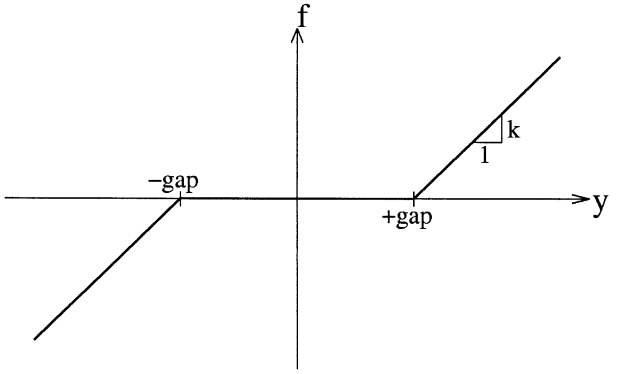

Fig. 8. Gap force model.

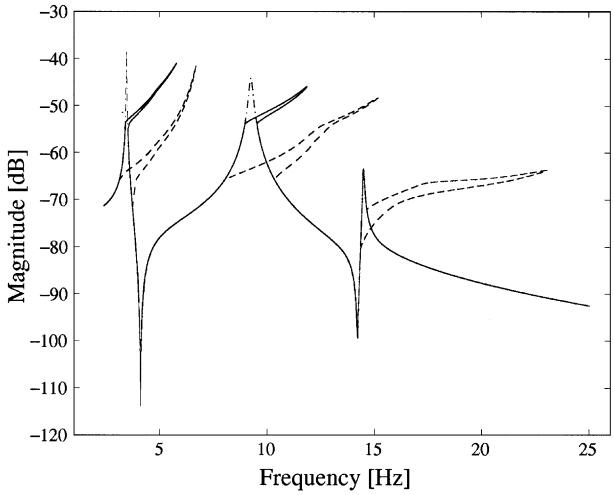

Fig. 9. Frequency response magnitude H_{11}^{11} for 0.1 N (– –) force, for 1.0 N (–) force and for 4.0 N (–·–) force (related to the structure of Fig. 7).

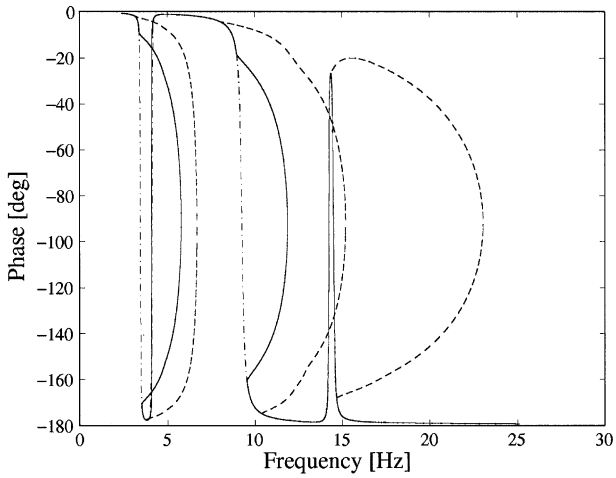

Fig. 10. Frequency response phase H_{11}^{11} for 0.1 N (– –) force, for 1.0 N (–) force and for 4.0 N (–·–) force (related to the structure of Fig. 7).

5. Concluding remarks

The frequency response curves of nonlinear dynamic problems are difficult to obtain through numerical simulations due to effects such as jump phenomena, snap-through and snap-back behaviors. Most classical numerical procedures such as Newton–Raphson or modified Newton–Raphson are not able to deal with limit points and fail in problems with these features.

In order to predict a complete nonlinear frequency response curves with jumps, snap-through and snap-back, the application of the arc-length method has been investigated in this work.

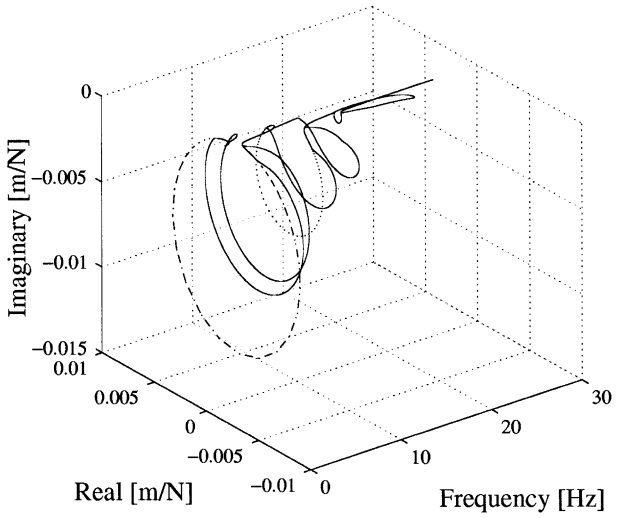

Fig. 11. Frequency response H_{11}^{11} for 0.1 N (––) force, for 1.0 N (–) force and for 4.0 N (–·–) force (related to the structure of Fig. 7).

The arc-length method is usually applied in nonlinear structural static and dynamic problems such as those with large displacements and large strain. The arc-length is able to deal with limit points in most typical nonlinear problems depending on the choice of some intrinsic parameters of the method such as the radius that defines the constraint equation.

The typical frequency response curves of nonlinear dynamic systems present some features such as severe inflection points, multiple solutions, etc., which causes difficulties even when using the arc-length method.

No particular difficulties has been detected during the predictor phase of the arc-length method. The stiffness determinant sign criterion worked as expected. On the other hand, many problems arises from the angle criterion adopted to choose the right iterative frequency factor. Even though great success has been achieved in most cases tested, difficulties are still encountered in some analysis when the radius was considered fixed. Using the automatic incremental of the radius solved the problem.

The results obtained in this work show that the arc-length can be applied with success to this class of problems. Some refinements of the method can be performed in order to increase the robustness, for example, new criteria for choosing the root sign of the frequency factor parameter.

References

[1] M.A. Dokainish, K. Subbaraj, A survey of direct time-integration methods in computational structural dynamics: I explicit methods, *Computers and Structures* 32 (1989) 1371–1386.

[2] M.A. Dokainish, K. Subbaraj, A survey of direct time-integration methods in computational structural dynamics: II, implicit methods, *Computers and Structures* 32 (1989) 1387–1401.

[3] M. Stylianou, B. Tabarrok, Finite element analysis of an axially moving beam, part I: time integration, *Journal of Sound and Vibration* 4 (178) (1994) 443–453.

[4] J.V. Ferreira, D.J. Ewins, Non-linear receptance coupling approach based on describing functions, in: *14th IMAC*, 1996, pp. 1034–1040.
[5] R.M. Lin, Non-linear coupling analysis based on a describing function, *Master's Thesis*, Department of Mechanical Engineering, Imperial College, London SW7 2BX, 1998.
[6] K. Murakami, H. Sato, Vibration characteristics of a beam with support accompanying clearance, *ASME Journal of Vibrations and Acoustics* 112 (15) (1990) 508–514.
[7] O. Tanrikulu, Forced periodic response analysis of non-linear structures for harmonic excitation, *Master's Thesis*, Department of Mechanical Engineering, Imperial College, London SW7 2BX, 1991.
[8] O. Tanrikulu, B. Kuran, H.N. Ozguven, M. Imregun, Forced harmonic response analysis of non-linear structures, *AIAA* 31 (7) (1993) 1313–1320.
[9] K. Watanabe, H. Sato, Development of non-linear building block approach, *ASME Journal of Vibrations, Stress, and Reliability in Design* 110 (1) (1988) 36–41.
[10] K. Watanabe, H. Sato, A modal analysis approach to non-linear multi-degrees-of-freedom system, *ASME Journal of Vibrations, Stress, and Reliability in Design* 110 (3) (1988) 410–411.
[11] E. Riks, An incremental approach to the solution of snapping and buckling problems, *International Journal of Solids and Structures* 15 (7) (1979) 529–551.
[12] M.A. Crisfield, A fast incremental/iterative solution procedure that handles "snap-through", *Computers and Structures* 13 (1981) 55–62.
[13] R. Lewandowski, Non-linear, steady-state vibration of structures by harmonic balance/finite element method, *Computers and Structures* 44 (1/2) (1992) 287–296.
[14] G.V. Groll, D.J. Ewins, The harmonic balance method with arc-length continuation in rotor/stator contact problems, *Journal of Sound and Vibration* 241 (2) (2001) 223–233.
[15] P. Sundararajan, S.T. Noah, Dynamics of forced nonlinear systems using shooting/arc-length continuation method—application to rotor systems, *Journal of Vibration and Acoustics* 119 (1997) 9–20.
[16] G.P. Tolstov, *Fourier Series*, Dover Publications, Inc., New York, 1976.
[17] J.J.E. Slotine, W. Li, *Applied Nonlinear Control*, Prentice-Hall, Inc., Englewood Cliffs, NJ, 1991.
[18] M.A. Crisfield, in: *Non-linear Finite Element Analysis of Solids and Structures*, Vols. 1, 2, Wiley, New York, 1997.
[19] K.J. Bathe, E.N. Dvorkin, On the automatic solution of non-linear finite element equations, *Computers and Structures* 17 (5–6) (1983) 871–879.
[20] G. Powell, J. Simons, Improved iterative strategy for non-linear structures, *International Journal for Numerical Methods in Engineering* 17 (10) (1981) 1455–1467.
[21] M. Papadrakakis, *Solving Large-Scale Problems in Mechanics*, Wiley, New York, 1993.
[22] P.G. Bergan, G. Horrigmoe, B. Krakeland, T.H. Soreide, Solution techniques for non-linear finite element problems, *International Journal for Numerical Methods in Engineering* 12 (11) (1978) 1677–1696.
[23] Y.T. Feng, D. Perić, D.R. Owen, Determination of travel directions in path-following methods, *Mathematical Computational Modelling* 21 (7) (1995) 43–59.
[24] M.J. Clarke, G.J. Hancock, A study of incremental-iterative strategies for non-linear analysis, *International Journal for Numerical Methods in Engineering* 29 (7) (1990) 1365–1391.
[25] W. Wagner, P. Wriggers, A simple method for the calculation of postcritical branches, *Engineering Computations* 5 (1988) 103–109.
[26] P.X. Bellini, A. Chulya, An improved automatic incremental algorithm for efficient solution of non-linear finite element equations, *Computers and Structures* 26 (1–2) (1987) 99–110.
[27] E.L. Allgower, K. Georg, Simplicial and continuation methods for approximating fixed points and solutions to systems of equations, *SIAM Review* 22 (1) (1980) 28–85.
[28] E. Riks, Some computational aspects of the stability analysis of non-linear structures, *Computational Methods of Applied Mechanical Engineering* 47 (3) (1984) 219–259.
[29] Z. Zhou, D.W. Murray, An incremental solution technique for unstable equilibrium paths of shell structures, *Computers and Structures* 55 (5) (1994) 339–348.